A case study: Improved imaging beneath the Cotton Valley formation through offset-dependent RMO picking and high-resolution tomography in the Lloyd Ridge area in the Gulf of Mexico

Taejong Kim, Francis Sherrill, Guy Hilburn, Yang He, and Cristina Reta-Tang, TGS*

Summary

This case study presents results from the Orion project within the Gulf of Mexico's Lloyd Ridge area. Difficulties arose in updating the velocity within the Cotton Valley Formation (CVF), a thin low-reflectivity layer of shale with carbonate stringers. The prestack depth migration (PSDM) common-image gathers (CIGs) and stack displayed noticeable undulations. To reduce the undulations, an offset-dependent residual moveout (RMO) picking technique was combined with high-resolution tomographic inversion to update the velocity model. This combined work flow resulted in a higher resolution velocity model, which enhanced the gather flatness and reduced the undulations of the event beneath the CVF layer.

Introduction

Imaging beneath heterogeneous carbonate formations is a formidable challenge. The latest imaging algorithms are suitable to the task, but require a velocity model resolution that is difficult to achieve for conventional reflection tomography. Cai et al. (2011), Xoawei et al. (2013), and El_Emam et al. (2013) proposed model-building solutions that all involve some degree of manual interpretation. Besides being time consuming, these approaches involved a prior assumption as to the shape of the structure in the absence of the anomalous carbonate layer.

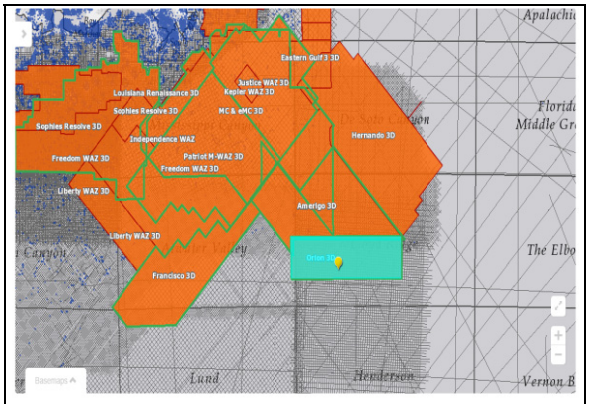

Figure 1: Map showing the location of the study area (cyan rectangle)

This case study area is composed of 175 OCS blocks (4100 square kilometers) in the Lloyd Ridge area in the Gulf of Mexico (Figure 1). The exploration potential includes Miocene structural and seismic attribute plays, Cretaceous carbonates and Jurassic Norphlet sand-salt roller plays, as well as deeper structural plays associated with the basement.

The objective of this study was to reduce the high-frequency undulations below the strongly inhomogeneous CVF layer (Figure 2). To flatten the undulations, it was essential to create a higher resolution velocity model.

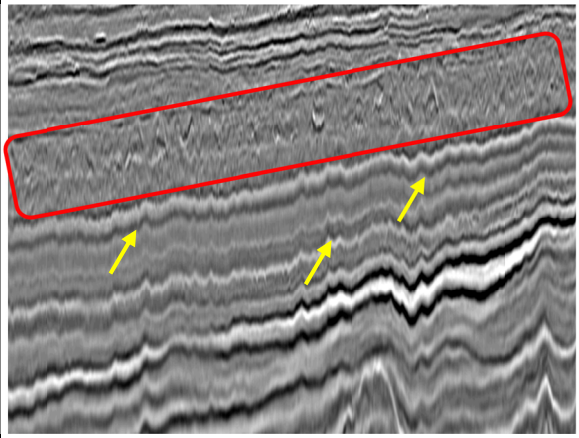

Figure 2: Events show undulations beneath the CVF layer (red box).

On investigation, the CIGs in this study were noted to display nonhyperbolic moveout (Figure 3). A single parameter (hyperbolic) or two parameter description of RMO were not adequate for the velocity model building for this project because of this problem. Therefore, the offset-dependent picking technique was recommended as input into the high-resolution tomographic inversion (Figure 3).

Offset-dependent Picking

When CIGs display moveout which coincides with low-order polynomial terms, polynomial-based RMO picking may effectively describe the smooth curvature. Industrial efforts have made great advancements in the use of this technique with real data (He and Cai, 2011; Bartana et al., 2011; Siliqi et al., 2007; Koren et al., 2008). In situations where the curvature is complex, the polynomial assumption may often be inaccurate (Liu et al., 2010). Complicated areas, such as those with high anisotropy, or that show

DOI http://dx.doi.org/10.1190/segam2014-1495.1

heavy faulting, will often yield events with multiple turning points, which may actually be made worse by polynomial-based flattening. Offset-dependent techniques, such as the plane-wave destruction method described by Fomel (2002; Liu et al., 2010), offer an alternative to more simplistic methods, in areas which require higher resolution imaging. These schemes have become common in the past decade, as they enable an accurate fit to complex moveout, regardless of curvature properties.

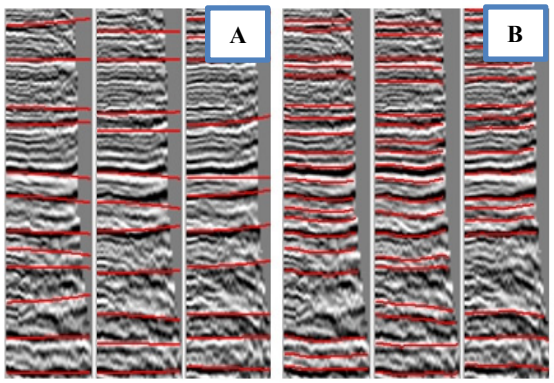

Figure 3: (A) One parameter picking; (B) Offset-dependent picking

In our offset-dependent picking method, the RMO is represented as a continuous displacement field rather than as a series of discrete events. A multiscale, constrained solver is used to estimate the displacement field for each CIG. The principle constraint is that the gradient of the displacement field (g) is less than some tolerance (T), where T is less than 1 (Hale, 2013).

$$|\nabla_z g(h,z)| < T \qquad (1)$$

This constraint prevents crossing events, and also waveform distortion caused by excessive stretching and squeezing. The events with maximum coherency are then computed from the derived displacement field. The advantage of this approach is that the computed events will be more consistent than if each event is estimated independently. This is important as exploration moves to increasingly complex targets such as subsalt, subbasalt, and other deep prospects.

High-resolution Tomography

Anisotropic Kirchhoff PSDM gathers were used. Super gathers are utilized to increase data signal-to-noise ratio (S/N) for more reliable analysis and picking of RMO for tomography. A supergather is computed by the following process:

- Collect CIGs in a patch;
- Estimate local dip using semblance scan;
- Align or shift traces based on the local dip;
- Stack the aligned common-offset traces in a patch area to form a supergather.

Using the offset-dependent picking technique, the RMO was scanned. These pick values, along with derived dip fields from the PSDM results, were input into the tomographic inversion. High-resolution model building is run on a dense grid of 100 m by 120 m (x and y), compared to conventional tomography on a 200 m by 200 m grid.

In addition, while polynomial-based tomographic inversion flattens curvatures, the offset-dependent tomography flattens moveout at each offset.

Figure 4 shows the dV overlaid on seismic image. It is remarkable to note that the perturbation patterns are highly correlated to the undulation of the events. It was important to keep the laterally-varying patterns for this study. Therefore smoothing was not applied to the dV in the CVF layer.

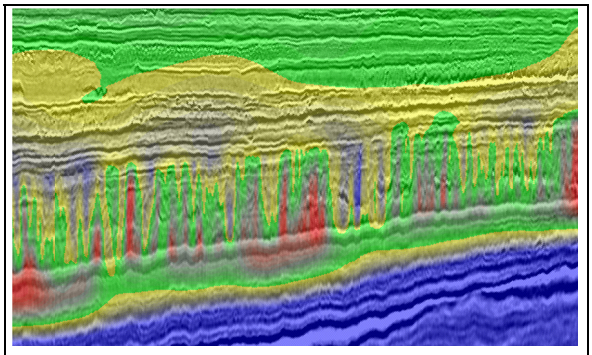

Figure 4: Velocity perturbation overlaid on the seismic image. Updated patterns are highly correlated to the undulation of PSDM image.

Figure 5 shows the velocity update (dV) from both types of tomographic updates, as well as the new velocities. In the CVF layer, the updated velocity (Figure 5D) is strongly inhomogeneous. To obtain the higher resolution velocity model in the CVF layer, a structure-conforming smoothing was applied to the dV. The structure-conforming smoothing was guided by horizons automatically picked on the PSDM image.

Figure 6 compares the PSDM gathers following the conventional velocity update to ones generated with high-resolution tomography combined with offset-dependent RMO picking technique. Figure 6B demonstrates that the gathers from the non-hyperbolic method are flatter, after one iteration.

DOI http://dx.doi.org/10.1190/segam2014-1495.1

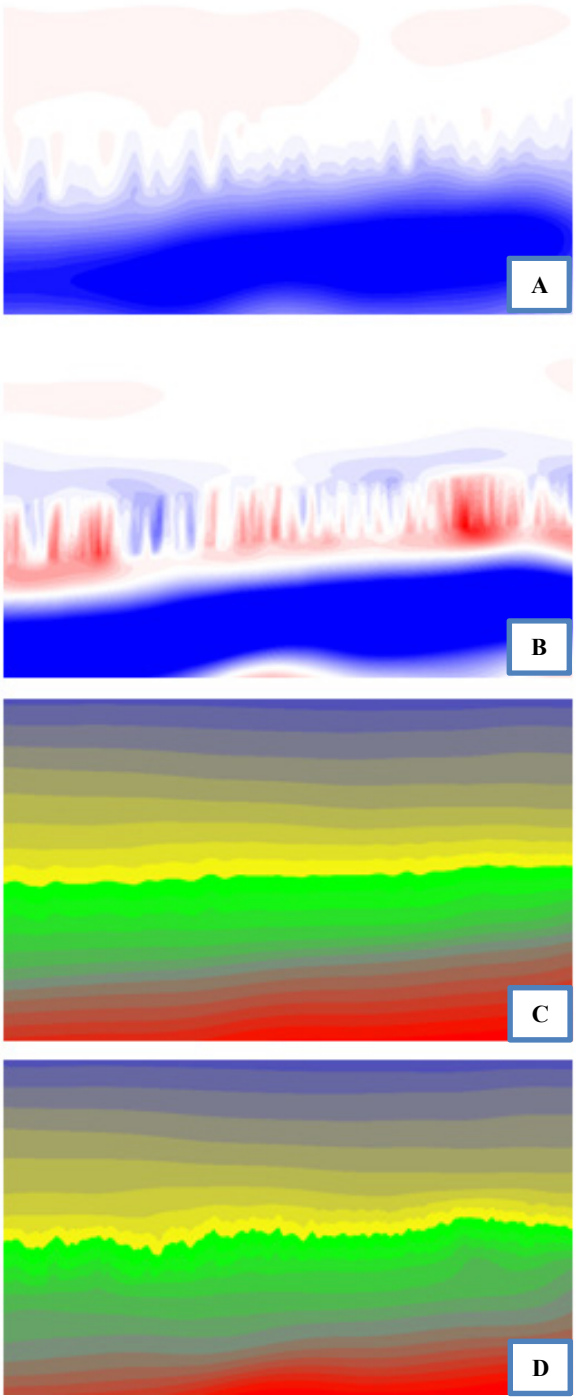

Figure 5: (A) Conventional tomography dV; (B) High-resolution tomography dV; (C) Conventional tomography sediment velocity; (D) High-resolution tomography sediment velocity

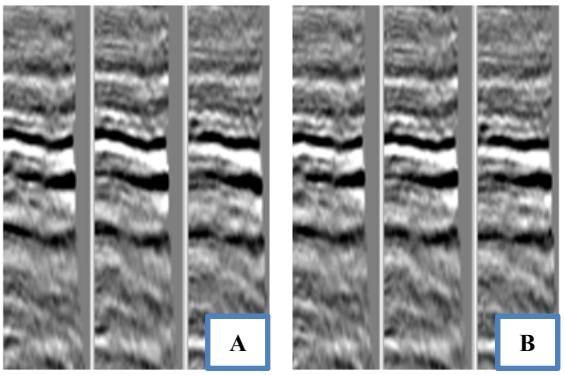

Figure 6: PSDM gathers; (A) Conventional update; (B) Offset-dependent picking and high-resolution tomographic update; The non-hyperbolic curvatures are flatter.

Figure 7 shows PSDM stacked images before and after tomographic updates. After the conventional tomography, the undulations of the reflections below the CVF layer are not reduced. However, the offset-dependent method reduced the nongeologic high frequency undulations superimposed on the events.

Finally, depth slices of the CVF layer with overlaid velocity models are presented in Figure 8. Figrue 8C shows that the update not only reduces the undulations of the reflections, but also captures the complicated heterogeneous structures.

Conclusions

The enhanced-velocity model building flow for this study included offset-dependent residual moveout picking, and a high-resolution tomographic inversion. This methodology yielded a higher resolution velocity model which was correlated to the strong lateral inhomogeneous structure in the CVF layer. Consequently, the events beneath the layer were flatter, and more geologically plausible than the events imaged with a velocity model updated with conventional techniques.

Acknowledgments

The authors would like to thank Xinyi Sun, Shiv Singh Simon Lopez-Mora, Bin Wang, and Zhiming Li for their valuable contributions during the project. We thank the management of TGS for permission to publish this study results and images. The authors thank Connie VanSchuyver's group for proof reading.

DOI http://dx.doi.org/10.1190/segam2014-1495.1

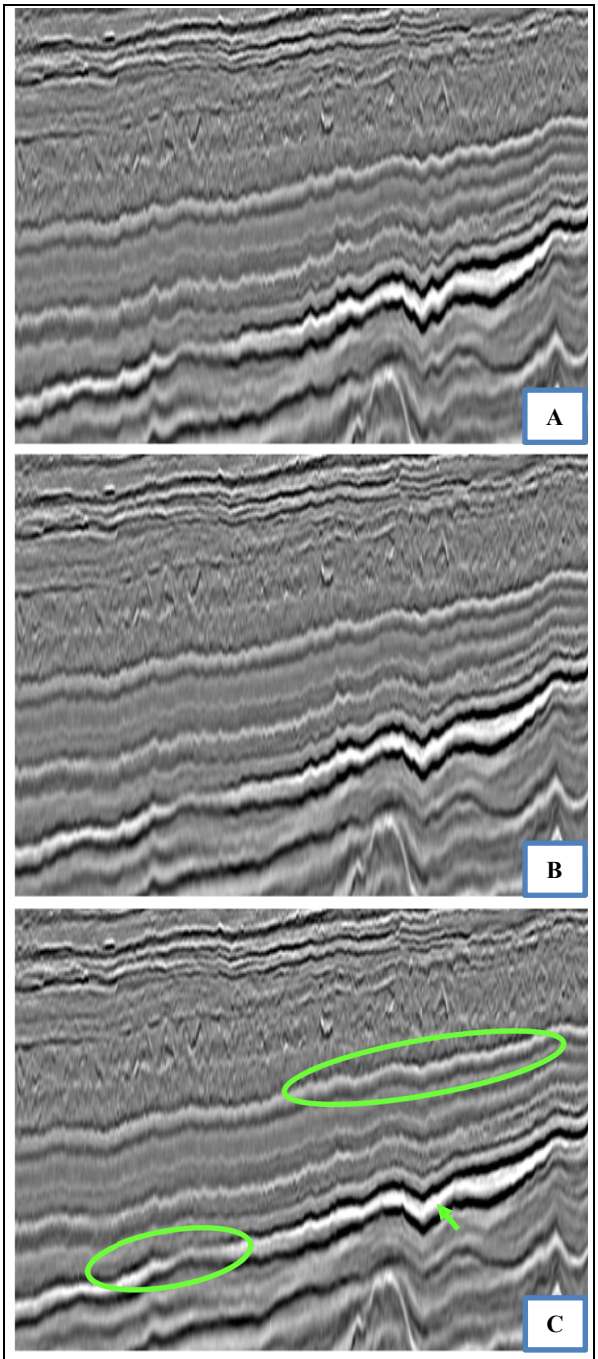

Figure 7: (A) Before velocity update; (B) Conventional velocity update; (C) Offset-dependent picking and high-resolution tomographic update; The conventional velocity update did not reduce the nongeologic undulations beneath the CVF layer, while the new update was much more successful.

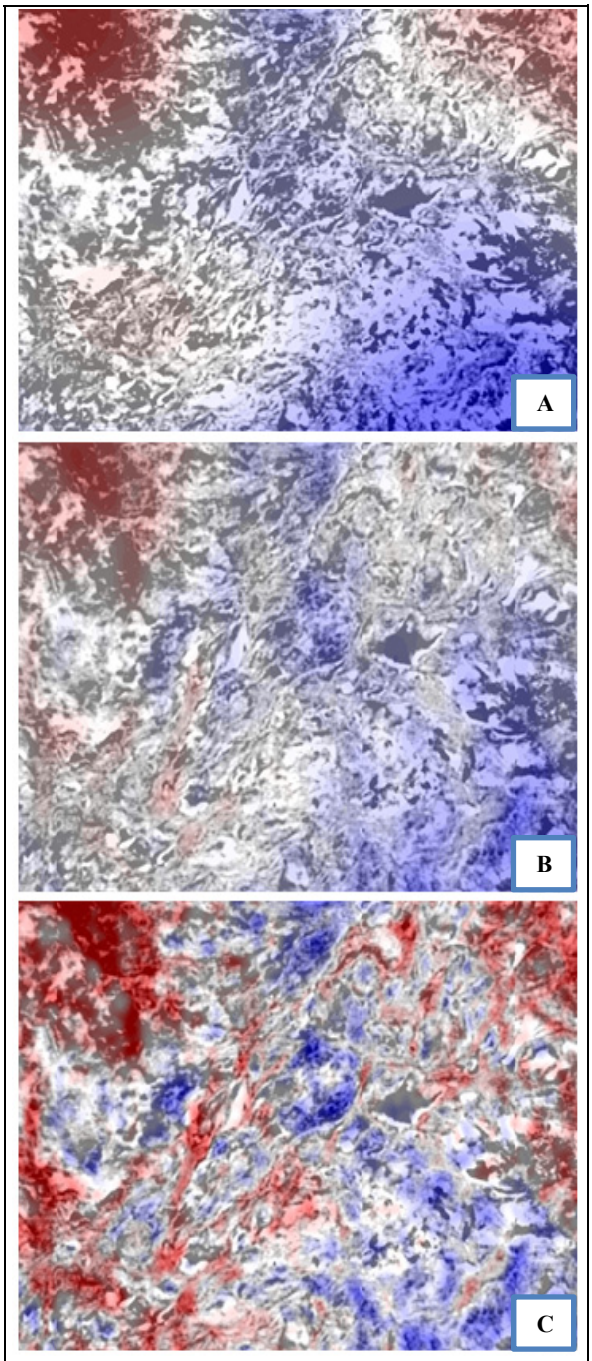

Figure 8: (A) Before velocity update; (B) Conventional velocity update; (C) Offset-dependent picking and high-resolution tomographic update; The velocity (C) was updated along the complicated heterogeneous structures.

DOI http://dx.doi.org/10.1190/segam2014-1495.1

http://dx.doi.org/10.1190/segam2014-1495.1

EDITED REFERENCES

Note: This reference list is a copy-edited version of the reference list submitted by the author. Reference lists for the 2014 SEG Technical Program Expanded Abstracts have been copy edited so that references provided with the online metadata for each paper will achieve a high degree of linking to cited sources that appear on the Web.

REFERENCES

Bartana, A., D. Kosloff, and Y. Hollander, 2011, Automatic picking of delays on 3D angle gathers: 81st Annual International Meeting, SEG, Expanded Abstracts, 3903–3907.

Cai, J., and H. Xun, Y. He Z. Li, S. Dong, M. Guo, and B. Wang, 2011, Detailed velocity model building in a carbonate karst zone and improving subkarst images in the Gulf of Mexico: 81st Annual International Meeting, SEG, Expanded Abstracts, 3280–3284.

El-Emam, A., A. Ebaid, W. Zahran, and B. Al-Ajmi, 2013, Delineation of karsts, a new approach using seismic attributes — Case study from Kuwait: 83rd Annual International Meeting, SEG, Expanded Abstracts, doi: 10.1190/segam2013-0927.1.

Fomel, S., 2002, Applications of plane-wave destruction filters: Geophysics, **67**, 1946–1960, http://dx.doi.org/10.1190/1.1527095.

Hale, D., 2013, Dynamic warping of seismic images: Geophysics, **78**, no. 2, O33–O43, http://dx.doi.org/10.1190/geo2012-0331.1.

He, Y., and J. Cai, 2011, Anisotropic tomography for TTI and VTI media: 81st Annual International Meeting, SEG, Expanded Abstracts, 3923–3927.

Koren, Z., I. Ravve, G. Gonzalez, and D. Kosloff, 2008, Anisotropic local tomography: Geophysics, **73**, no. 5, VE75–VE92, http://dx.doi.org/10.1190/1.2953979.

Liu, J., and W. Han, 2010,Automatic event picking and tomography on 3D RTM angle gathers: 80th Annual International Meeting, SEG, Expanded Abstracts, 4263–4268.

Siliqi, R., P. Herrmann, A. Prescott, and L. Capar, 2007, High-order RMO picking using uncorrelated parameters: 77th Annual International Meeting, SEG, Expanded Abstracts, 2772–2776.

Xiaowei, W., Y. Gang, T. Yancan, L. Lei, and Q. Shuhai, 2013, Analysis of factors affecting carbonate fracture-cave imaging: 83rd Annual International Meeting, SEG, Expanded Abstracts, doi: 10.1190/segam2013-0318.1.